UA2 TRIGGER AND DATA ACQUISITION

V. Hungerbühler, CERN

UA2 Collaboration (Bern, CERN, Copenhagen, Orsay, Pavia, Saclay)

The UA2-detector mainly consists of a track detection system without magnetic field, surrounded by calorimeters. While it is primarily designed for the detection of the electron-decays of the W and Z bosons at the $p\bar{p}$ collider, it can explore a whole range of other physics, such as inclusive particle production, jets, neutral over charged energy ratio, etc... The main triggers are formed by adding the analog signals from the electromagnetic calorimeters to "energy" clusters and applying a threshold to them. These clusters are also converted to digital values in 2.5 μsec, and are available for more sophisticated triggering with a processor which may be added later. The data acquisition is done by means of a VAX 11/780 through a ROMULUS/REMUS system. Four minicomputers can simultaneously "spy" on part of the data acquired by the VAX. During beam-off periods, parts of the detector electronics can be decoupled from the VAX and be put under control of a minicomputer. Thus several detector parts can be simultaneously and independently debugged.

1 - INTRODUCTION

The injection of cooled antiprotons into the SPS[1] and their acceleration to 300 GeV opens up the possibility of studying $p\bar{p}$ collisions at a centre-of-mass energy $\sqrt{s}$ = 600 GeV where many new phenomena are expected to occur.

In particular with a luminosity $L \cong 10^{30}$ cm^{-2} s^{-1} it becomes possible to produce a significant number of $W^{\pm}$ and Z^0, the weak intermediate bosons of unified gauge theories, if their production cross section is of the order of a few 10^{-33} cm^2 as predicted by current QCD calculations.

This contribution limits itself to a description of those systems of UA2 where most of the real-time data processing occurs, i.e. the calorimeter trigger logic and the on-line computers.

It has been a major concern to keep the trigger as compact, simple and reliable as possible. Although microprocessors are increasingly being used as trigger processors in high energy physics experiments, UA2 has chosen to take advantage of the compactness of analog electronics for the major part of its trigger. The digital part is mostly implemented with the powerful MBNIM-standard[2] which is at once compact and economical, modular, flexible and fast.

The large size of the collaboration and particularly the fact that each major detector part is built by a different collaborating institute, have naturally led to the use of several on-line minicomputers in addition to the main on-line computer, a VAX 11/780. During data acquisition, they can monitor "their" detector by "spying" on part of the data acquired by the VAX. During beam-off periods, a single switch allows to decouple a part of the detector electronics from the VAX and to put it under control of the associated minicomputer. Thus up to 5 detector parts can be simultaneously and independently debugged.

2 - THE EXPERIMENTAL APPARATUS

The detector[3] is largely dedicated to the observation of the hadronic and leptonic decay modes of the weak vector bosons ($W^{\pm}$, Z^0). Nevertheless, the resulting apparatus is very suitable for the detection of other expected -or unexpected- phenomena.

A constant and major concern has been to maintain simplicity and compactness in the design, as imposed by the constraint of operating the detector in the difficult environment of the SPS tunnel.

For this reason, and because of the good energy resolution obtainable in lead-scintillator sandwich counters, we have concentrated on the electron rather than the muon decay modes of the $W^{\pm}$ and Z^0. Electron identification is therefore instrumented over nearly 4πsr by lead-scintillator sandwich counters.

A drawing of the entire detector is presented in Fig. 1. At the centre of the apparatus is the vertex detector which will measure particle trajectories to an accuracy of about 200 μm in all 3 projections in a region free of magnetic fields. It consists of 4 multiwire proportional chambers with cathode strip readout, a cylindrical scintillator hodoscope and 2 jade-type drift chambers with charge division and multihit readout. These detectors are surrounded by a converter of 1.5 radiation lengths of tungsten followed by another multiwire proportional chamber. In the central region, covering ±1 rapidity unit about 0, the vertex detector is surrounded by lead-scintillator sandwich counters followed by hadron calorimeters. The calorimeter assembly consists of 240 independent cells, each cell (Fig. 2) covering 15° in azimuthal and 10° in polar angle. This is a compromise between minimizing dead space and providing sufficient space resolution. Light is collected with BBQ-doped wavelength shifting light guides. Each compartment is viewed with 2 light guides and 2 photomultipliers to provide information on the position of the shower so that light collection efficiency corrections can be made.

The polar angular regions of 20° to 37.5° and 142.5° to 160° are each instrumented with a toroidal magnet consisting of 12 coils. The average field integral along particle trajectories is .38 Tm. Each region between two adjacent toroid coils is followed by a set of 9 drift chamber planes with an average lever arm of 80 cm. Together with the vertex detector, these forward/backward (F/B) chambers allow reliable charge measurements on electrons up to 60 GeV/c transverse momentum. Each drift chamber set is followed by a converter of 6 mm Pb and proportional tubes for an accurate measurement of the position of electromagnetic showers. This allows an improved rejection of the overlap background (a low momentum hadron track near a π^0, simulating an electron in the calorimeter that follows) and a better hadron rejection. The proportional tubes are followed by the F/B calorimeters, consisting of lead scintillator sandwiches and covering the same solid angle as the toroid magnets. There are 12 forward and 12 backward calorimeter sectors, each subdivided into 10 cells that cover 15° in azimuthal and 3.5° in polar angle. Each cell consists of 24 radiation lengths of lead scintillator sandwich, followed by a 6 radiation length lead scintillator sandwich used as a hadron veto. Each compartment is viewed with 2 photomultipliers.

The momentum measurement of charged secondaries in the central region would permit

the measurement of charged particle inclusive production, and greatly benefit the study of jet structure at large transverse momentum, free quark production, etc... To this end a 30° azimuthal window will be opened in the calorimeter in the first phase of operation of the detector and equipped as a magnetic spectrometer. The use of the calorimeter iron as the return yoke of the magnetic spectrometer allows a very compact geometry. Electron identification remains possible in the azimuthal wedge because of the presence of a large lead-glass wall behind the magnetic spectrometer. The field integral is of the order of 1 Tm. This "wedge detector" (Fig. 3) consists of 12 large drift chamber planes, a 28 counter scintillator hodoscope for time-of-flight measurements, a shower counter consisting of 2 cm of iron followed by another 28 counter scintillator hodoscope and a lead-glass wall which is 28 (15 cm x 15 cm) blocks wide, 10 blocks high and 14 radiation lengths deep.

In the symmetric configuration the total acceptance is ≅ 63% for $Z^0 \to e^+e^-$ and ≅ 75% for $W^{\pm} \to e^{\pm}\nu$; it is independent of the p_T-distribution of the produced boson, up to at least $\langle p_T \rangle$ = 10 GeV/c. Thus, with a Z^0 production cross section of 2 x 10^{-33} cm^2 and a leptonic branching ratio of 3 %, .14 detected $Z^0 \to e^+e^-$ per operating hour are expected. The mass resolution at the Z^0 peak is expected to be ≅ 1.5%.

3 - THE CALORIMETER TRIGGER

The trigger algorithms are largely dictated by the properties of the detector and by the physics events that are to be detected. A major simplification of the trigger is achieved by the calibration of the calorimeter cells in transverse energy rather than energy. Since the event rates primarily depend on transverse momentum and since each calorimeter cell subtends about the same $\Delta\phi\,\Delta y$ solid angle, a single common threshold results in similar trigger rates in any cell, independent of its position.

The Z^0 and $W^{\pm}$ -triggers are based exclusively on the electromagnetic calorimeters. The hadronic compartments only participate in very simple triggers, such as total transverse energy. Fig. 4 shows the development of the e.m. calorimeter cells in the θ-ϕ plane. Each square corresponds to a cell. In the central calorimeter, cells are adjacent to their neighbours ; the physical gap between neighbouring cells is less than 1 mm. However, in the forward/backward calorimeters each of the 12 sectors is separated from its neighbours by typically 15 cm due to the shadow of the toroid magnet coils. There are 480 electromagnetic cells, involving 960 photomultipliers.

The transverse dimensions of the calorimeter cells are rather small, especially in the central calorimeter where they are typically 10 cm x 10 cm. Thus, there is an appreciable probability that an electromagnetic shower is shared among several neighbouring cells. Applying a threshold to each individual cell would result in a serious trigger inefficiency. Trigger thresholds must be applied to sums of neighbouring cells, i.e. to cell clusters. To this end, all possible 2 x 2 cell clusters are formed, indicated by crosses in the upper half of Fig. 4. In the central calorimeter, each cell participates in 4 such sums, namely at each of its corners. An exception are the edge-cells in θ, which contribute to only 2 clusters. In the F/B calorimeters, four 2 x 2 clusters are possible in each sector. Adjacent

sectors are not added since they are physically separated. Thus 480 e.m. cells are summed up to 312 clusters.

Fig. 5 shows an example of the effect of the clustering. The upper half presents a possible configuration of energy deposits in the cells (or modules), with sharing among neighbours. Fig. 5b shows the result of the clustering algorithm. There are always more non-zero clusters than there were non-zero cells. In the case of a single isolated cell, 4 neighbouring clusters of exactly the same height are generated.

Requiring at least one cluster above a given common threshold now results in a very efficient trigger for electromagnetic showers above a given transverse momentum. For certain applications, such as multiplicity counting, it is desirable to exclude all the spurious clusters around any detected peak. This is indicated in the lower part of Fig. 4. Provisions are made in the hardware to first detect the largest clusters and to subsequently veto their neighbours. In the case of 2 neighbouring clusters of the same size, they are both accepted.

The trigger algorithms are implemented in the hardware with 2 modules, called OLIFAN and ROLAND. The diagram in Fig. 6 shows the use of one-tenth of the OLIFAN module. The signals of the 2 photomultipliers of each cell are transported by 80 m long coaxial cables to a linear fanout of gain 1. In order to increase the dynamic range of the LRS 2282E integrating ADCs, two channels are used for each e.m. photomultiplier, one receiving the non-amplified signal and the other one a signal amplified by a factor 12. The signals of the 2 photomultipliers associated to the same calorimeter cell are also linearly added and then held in an integrating sample-and-hold (ISH). After gating, the ISH outputs a d.c. voltage which is proportional to the summed charge from the cell, 100 mV corresponding to about 1 GeV of transverse energy. This voltage is kept constant to better than 20 mV over 3 μs. This introduces appreciable errors at very low cluster energies, but they become completely negligible at the threshold levels of interest. The ISH is linear to about 2.5 V. Above 25 GeV, it saturates without any ill effects on the trigger since any cluster above 25 GeV will always represent a good trigger. Fig. 6 also indicates the test system which allows to inject a variable known charge into each photomultiplier channel. It is used both for measuring the linearity and the gain of the fanout-ADC chain and for testing the trigger system.

The 2U-wide CAMAC-type OLIFAN-module contains 20 linear fanouts, 20 amplifiers and 10 ISH, enough to satisfy the needs of the electromagnetic layer of a single "orange slice" (the 10 central calorimeter cells at constant ϕ). The amplifiers and ISH are built on separate small printed circuits which can be inserted with connectors on the main printed board. Thus, the OLIFANs can also be used for the hadron calorimeter cells where no ISH nor amplifiers are needed. The OLIFAN is primarily a receiver and fanout-module ; it participates in the trigger algorithm only insofar as it adds the 2 photomultiplier signals of each cell and prepares them for the trigger by integrating them.

It should be noted that the timing of the UA2-trigger is different from what is current at fixed-target machines. Since the bunches in the $\bar{p}p$-collider cross each other every 4 μs in about 2-3 ns, the time of the potential events is very well defined, and in advance. Thus it is possible to gate the ADCs, memories, etc... at every beam crossing time without waiting

for a trigger, saving space and money on delay cables. UA2 then allows about 800 ns for a first level trigger to determine if the event that has just been gated is to be kept or not. If no, a general reset-signal is issued so that the electronics can be ready for the next potential event. This trigger timing introduces no dead-time at all ; of course, the resetting times of all electronic modules must be below 3 μs.

The trigger module ROLAND and the associated digital logic take advantage of the ample time allowed by the 4 μs beam crossing interval, by taking several decisions in sequence in the hardware. In this sense it approaches the functions of a digital processor, but it still retains the speed of the fast electronics. It is considerably more flexible than normal NIM-electronics, but still much less than a general purpose processor.

The front-end of the ROLAND sums the adjacent cells up to clusters. Fig. 7a shows the resistor network which distributes the currents from a single ISH in the OLIFAN to the 4 clusters in which every cell participates. Each ROLAND, like the OLIFANs, is associated to a single "orange slice" or rather to a row of clusters between 2 adjacent "orange slices". Since each cell participates in 2 different rows of clusters, its d.c. voltage is needed in 2 adjacent ROLAND-modules. The distribution is accomplished by a short cable which leaves the first ROLAND at "CL OUT" and enters the neighbouring ROLAND at "CL IN". The resistors are chosen in such a way that this cable sees $Z_c = 100\Omega$ at the input "CL IN". Fig. 7b indicates how the clusters are formed, namely from the input signals which the ROLAND gets from its associated OLIFAN plus the signals which it receives from its neighbour. At the same time it sends a copy of its input signals to its other neighbour. The front panels of the two modules as well as some of the interconnections are shown in Fig. 8.

Each summed d.c. voltage corresponding to the cluster energy can now be compared with a reference voltage, as indicated in Fig. 9. V_{ref}, which is common to all 9 clusters of a ROLAND and which may even be common to many modules, is generated by a fast 8-bit DAC (less than 10 ns settling time) controlled by a synchronous counter. A one-bit step of the DAC corresponds to about 100 MeV of transverse energy. Loading any digital value into the counter results in applying a common threshold to all clusters. Any cluster exceeding this threshold sets its associated flip-flop. The state of all flip-flops is communicated to the outside world through a standard MBNIM-connector. The decision of whether a trigger is present or not at this given V_{ref}-threshold is then based on the configuration of all the flip-flops of which there are as many as possible clusters. The OR of the 9 flip-flops in a ROLAND-module is also available as a NIM-output. Several thresholds can be applied in sequence at a rate of one every 100 ns.

In addition, the ROLANDs can be used as fast ADCs, capable of converting all clusters simultaneously to 8-bit numbers in 2.5 μs. To this end the synchronous counter is loaded with the highest value possible and then let count down. Any time a comparator changes its state from zero to one its flip-flop is set, vetoing any further clocking of the flip-flop. Simultaneously a shift register is loaded with the value of the counter, thus memorizing the digital value of the cluster energy. The counter value is converted to Gray code before memorization in order to avoid errors due to synchronisation problems. As indicated in Fig. 8 and 9, the vetoing of the spurious clusters around a detected peak (Fig. 4) is

implemented by ANDing the complement of the set flip-flop with the clocks of the neighbouring flip-flops, provided that the veto-cabling between adjacent modules is present.

4 - THE DIGITAL TRIGGER LOGIC

When the synchronous counters of the ROLANDs have reached zero, the shift registers contain the digital values of all clusters or only those of all peaks if the veto logic is used. The shift registers can be read out by a non-standard crate controller which reconverts the Gray-code values into binary words and sends them to the ROMULUS/REMUS readout system[4] in the standard format. The reading time is of the order of 200 μs. Presently it is envisaged to convert all clusters and to read them as part of the event. They will be used on-and off-line to check on the correct functioning of the trigger logic and possibly as an aide to the pattern recognition in the e.m. calorimeters.

It is also possible, although at present not yet foreseen, to transfer the contents of the ROLAND shift registers to a second level trigger processor which could apply more sophisticated trigger algorithms, such as calculating invariant masses among the biggest clusters etc... With a modified version of the crate-controller it would be possible to read out the registers in as little as 20 μs. In this case it would also be an advantage to use the veto logic so that the trigger computer would spend no time on processing spurious clusters.

Fig. 10 shows the timing of the UA2 trigger. After gating the ADCs and the ISH, a first threshold is applied to all ROLANDs and a test is made if at least 2 clusters above threshold are present. If this so-called "Z"-trigger is satisfied, it is recorded in a MBNIM strobed coincidence register, used as a memory. In any case, a second, higher, threshold is applied about 100 ns later, and at least one cluster is required to set the so-called "W"-bit. While the trigger bit register is open, other bits corresponding to certain multiplicities, large total energies in the hadronic and/or e.m. calorimeters, various wedge triggers etc... may be set at any time. After 800 ns, a decision is taken on whether to keep or to reject the event, based on the configuration of the trigger bits and on a computer-defined trigger-enable mask. If the event satisfies the trigger, all clusters are converted to digital values in 2.5 μs by the application of a linearly decreasing V_{ref}, before reading out the event. The number and values of the different thresholds applied inside the ROLANDs are controlled digitally by a table in a CAMAC-module (DURANDAL) which itself is loaded by computer. Up to 16 different thresholds and/or slopes can be programmed, giving a lot of flexibility.

The algorithm requiring an electron pair is more sophisticated than just demanding 2 clusters above threshold, since 2 clusters which are close together in solid angle represent relatively small masses and are likely to dominate the trigger rate. Thus, we require that the 2 e.m. clusters are separated in azimuth by an angle of the order of 90 degrees. For this purpose, the OR of all clusters at a given ϕ is formed, leaving 24 binary variables corresponding to 24 ϕ-values. This is easy to implement in the hardware since the ROLANDs

already generate it for the central calorimeter ; only the OR between the central and the F/B calorimeters needs to be made. The coincidence condition is illustrated in the upper part of Fig. 11. The half-circles opposite each hit (cross) represent the ϕ-region which any other hit has to occupy in order to form a valid electron-pair trigger with the first hit. The lower half of Fig. 11 indicates the way the coincidence pattern is implemented. If a device is available which allows to generate for any hit the predicted bit pattern of second hits which may form a valid coincidence with the first one, the work is almost done. All there is left to do, is to form the bit-by-bit AND between the original bit pattern and the OR of all predicted bit patterns and to require that at least one bit is set. Such devices exist within the MBNIM-standard[2].

MBNIM has been developed at CERN by F. Bourgeois and his collaborators ; it represents a real step forward in fast digital nuclear electronics. Its most distinguishing feature is a flat cable bus consisting of 16 signal lines, 2 synchronization lines and one control line carrying ECL signals at up to 100 MHz. Both output ORing and input bussing are possible, with a fanout of up to 10. At least ten different NIM and CAMAC modules following the MBNIM-convention exist, many of them available at the CERN-EP Electronics Pool. They can be considerably more economical than standard modules, based on coaxial interconnections : on one hand, the MBNIM cable is a bus, eliminating very often the need for fanouts and multiple cables, on the other hand, MBNIM can be made more dense, since they are not as much limited by the space on the front panel as with coax connectors. Also less chips are needed inside the modules because no NIM-ECL conversions and vice-versa need be done.

A highly useful MBNIM-module for coincidence matrices is the BIT-ASSIGNER (Fig. 12), a 2 U wide CAMAC-unit. Logically, it consists of 16 registers of 16 bits which can be loaded by CAMAC-operations. Any input bit which is present selects its associated 16-bit register : the output is the OR of all selected registers. This unit can operate at above 20 MHz. Using the output ORing and input bussing capability of MBNIM, the bit-assigner can be extended to 32, 48, 64 bits etc..., at the expense of more modules, i.e. 4, 9, 16, etc...

For the electron-pair trigger, a bus of 24 bits is needed ; thus a 32 bit wide bus and 4 bit-assigners are used. The full logic diagram of the e.m. calorimeter trigger logic is shown in Fig. 13. Four strobed coincidence registers (SCR) convert the NIM-levels of the ROLAND-OR-outputs to a 32-bit wide bus (busses 1A and 1B) of which 24 bits are used. At the same time, this bus produces the OR between the central and F/B calorimeter cluster patterns. The bit-configuration of bus 1 is memorized in a 32-bit pattern unit (MISTER), which also generates the OR of all bits. The NIM-output makes the "W"-trigger in coincidence with the W-strobe which arrives when the "W"-threshold level is applied and stable. Four bit assigners (BA) generate the predicted 32-bit pattern (busses 2A and 2B) for the "Z"-trigger. The 2 arithmetic-logic-units (ALU) form the bit-by-bit AND between busses 1 and 2. A "Z"-trigger is generated if any bit of the coincidence is non-zero at the time the Z-strobe arrives. The SCRs must be cleared between the Z- and W-trigger levels and then be strobed again. The TERMINIM-modules are included only for convenience in the debugging of the system. If the TERMINIMs were left out, the bus terminations (indicated by dots at the end of the busses) could be incorporated in the pattern unit. Not shown in Fig. 13, but foreseen, is the

extension of bus 1 to a MBNIM-scaler unit, MIMOSA, which contains 32 40 MHz scalers in a single width CAMAC module.

MBNIM-modules are used in other parts of the UA2 electronics, especially in the wedge trigger logic. There, 56 hodoscope signals and 13 signals from the leadglass modules are combined to generate triggers on electrons, charged hadrons, neutral electromagnetic showers and on less-than-minimum ionizing particles. This digital logic, not described here, could be implemented with standard NIM logic, available from the EP-Electronics Pool, at a cost of 80 KSF for the modules and the 3 crates which they would occupy. Instead, MBNIM-modules are used, also supplied by the EP-Electronics Pool, at a cost of 35 KSF. In addition, this logic only occupies 1 crate. In the case of the calorimeter trigger, a comparison is more difficult, since it is very cumbersome to realize the electron-pair algorithm in ordinary NIM-logic. A custom-made coincidence matrix would have to be built. Here, MBNIM offers the advantage of being readily available and of allowing an easy reconfiguration if the needs change.

5 - THE ON-LINE COMPUTERS

A general overview of the UA2 data acquisition system is shown in Fig. 14. Each square represents a major section of the data acquisition electronics, associated to a specific detector part, typically consisting of 5 to 15 CAMAC-crates. All crates are controlled and read through ROMULUS/REMUS crate controllers and branch drivers.

A VAX 11/780 with 2 Mb of memory and 140 Mb of disk space is the main on-line computer. In principle, only this computer is needed for data acquisition, tape writing and detector monitoring. Fig. 14 also shows the PDP 11 computer of UA4 as well as the UA4 electronics, since that experiment uses the UA2-vertex detector and will also make use of the VAX for data acquisition. The other 4 minicomputers are complete systems with typically 50-100 kb of memory, a disk and a CAMAC interface. They mainly serve two purposes : during beam-off periods, they can take over the detector parts to which they are associated for detector development and debugging. This allows to work independently with up to 5 detector parts and to greatly increase the efficiency and speed with which the apparatus can be brought on-line. During beam-on time, while the VAX takes data, they can spy on the data of "their" detector for monitoring. While the principle has been adopted that all important monitoring functions must be done on the VAX and that the data acquisition must work correctly independently of the states of any of the minicomputers, they are nevertheless very useful. The detailed, in-depth, diagnostic routines cannot all run simultaneously on the VAX. Thus, the VAX normally only runs overall monitoring routines. When any such task indicates a problem, special diagnostic programs to localize the fault have often to be called in, which take time to accumulate histograms. When the minicomputers are running, they can accumulate such detailed histograms on a permanent basis, thus shortening the intervention times in case of detector failures.

The event "spying" is done through a CERN-developed REMUS-module, a "router", indicated

by small rectangles on Fig. 14. UA2 uses two of its modes : In the "spying" mode, the data stream goes to the VAX. A minicomputer has no control over such a REMUS branch but it can get a copy of any passing event if it has requested it. In the "decoupling" mode, the VAX is completely decoupled from the corresponding REMUS branch, and the minicomputer is in complete control of the branch, such that it can initiate a data acquisition which is completely autonomous and asynchronous with respect to the other computers. In fact, this not only implies the control over the CAMAC- or REMUS- bus. It also requires that the computer be capable of enabling the gates to the electronics it is supposed to have under control ; it must receive interrupts, generate dead times and resets, etc... All these control lines which usually carry NIM-signals must also be switched from the VAX to the minicomputers or vice-versa. This is quite simply done by means of a NIM-module which contains 10 reed-relais and which can be switched by an external NIM level (Fig. 15). The manual router controllers which allow to change the mode of the routers are capable of producing this NIM control signal. Thus, it is possible to switch the full control of a REMUS-branch between the VAX and a minicomputer with a single switch, reducing the number of possible errors close to zero. Of course, this is only done at most a few times per day, since it generally involves the initialization of new programs on the computers.

UA2 uses nevertheless one small microcomputer, in an almost stand-alone configuration. It is a TMS 9900 microprocessor with 32 kb of memory, housed in a 2 U wide CAMAC module. It has been developed at CERN and is now commercially available as SEN 2103. It is used as the master of a single crate which contains up to 300 channels of scalers and a video display driver. Its task is to read the scalers periodically and to display the rates on several video screens. In addition, it can be adressed through a type A2 CAMAC crate controller. Thus, the VAX main computer is able to read rates accumulated by the TMS 9900 over several hours. For better reliability, the programs will be exclusively in EPROM.

ACKNOWLEDGEMENTS

I would like to thank P. Darriulat and A. Rothenberg for many useful discussions. Many thanks for helpful explanations go to F. Bourgeois who invented the MBNIM system and who developed with his team the OLIFAN- and ROLAND-modules and to G. Schuler who built, among others, the integrating sample- and -holds.

REFERENCES

1 - C. Rubbia, P. Mc Intyre and D. Cline, in Proceedings of the International Neutrino Conference Aachen 1976, ed. Faissner, H. Reithler, P. Zerwas (Vieweg, Braunschweig, 1977) ;

S. Van der Meer, CERN/SPS/423 (1978) ;

Design Study of a $p\bar{p}$ Colliding Beam Facility, CERN/PS/AA 78-3 (1978).

2 - A. Beer et al., MBNIM : A modular approach to fast trigger logic for high energy physics experiments, Nucl. Instruments and Methods 160 (1979) 217-225 ;

F. Bourgeois, Modular trigger logic techniques at the CERN OMEGA Spectrometer, paper presented at the Nuclear Science Symposium, San Francisco, 17-19 October 1979 ;

T. Armstrong et al., NIM 175 (1980) 543-547 ;

A. Corre et al., NIM 179 (1981) 585-590 ;

MBNIM-user guide, F. Bourgeois, ed., August 1980, available from the CERN-EP Electronics Pool.

3 - M. Banner et al., CERN/SPS/78-08 (1978)
and CERN/SPS/78-54 (1978).

4 - F. Bourgeois, Proposal for a large scale data acquisition system using CAMAC, CERN NP 75-4, 30 May 1975 ;

P.J. Ponting, Guide to ROMULUS/REMUS Data Acquisition Systems, EP-Electronics note 80-01, CERN (1980).

* * *

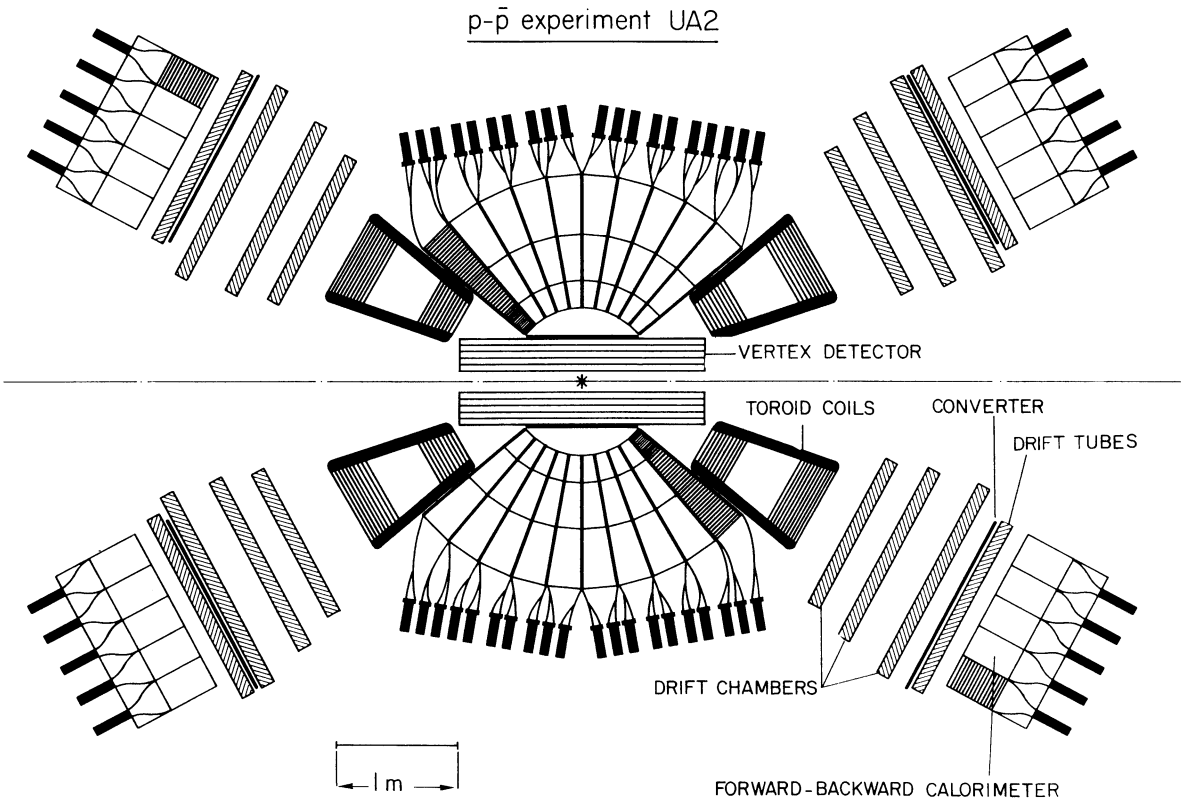

Fig. 1 : Cross section of the UA2-detector

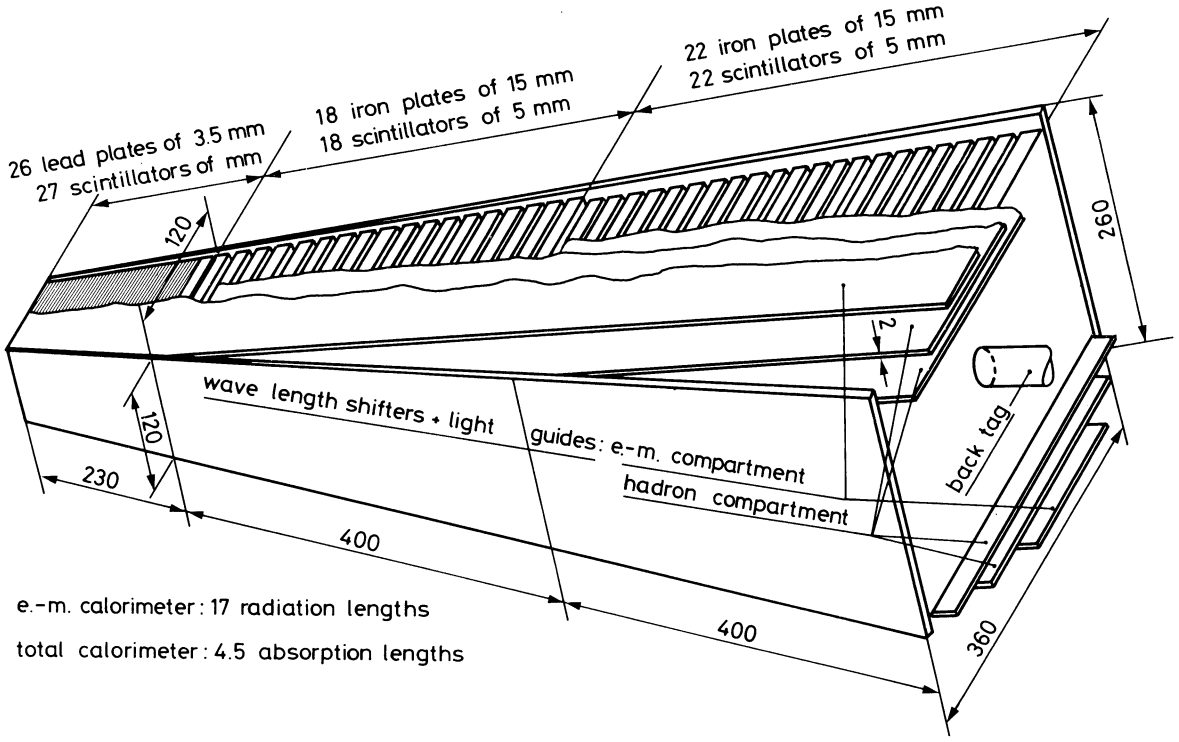

Fig. 2 One of 240 cells of the central calorimeter

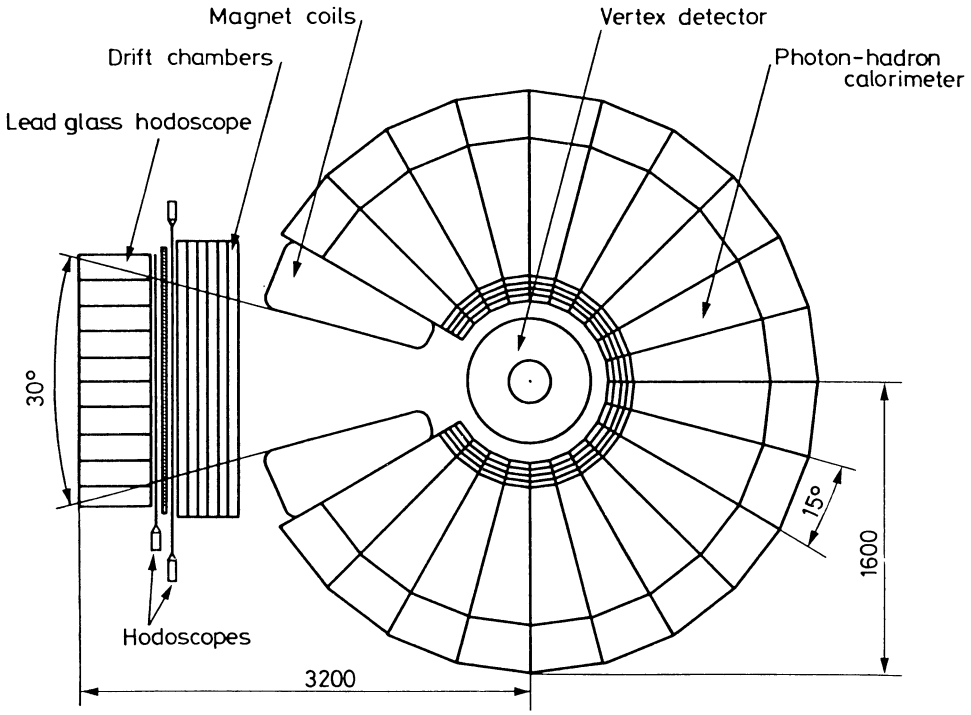

Fig. 3 Cross section of UA2 detector perpendicular to the beam axis

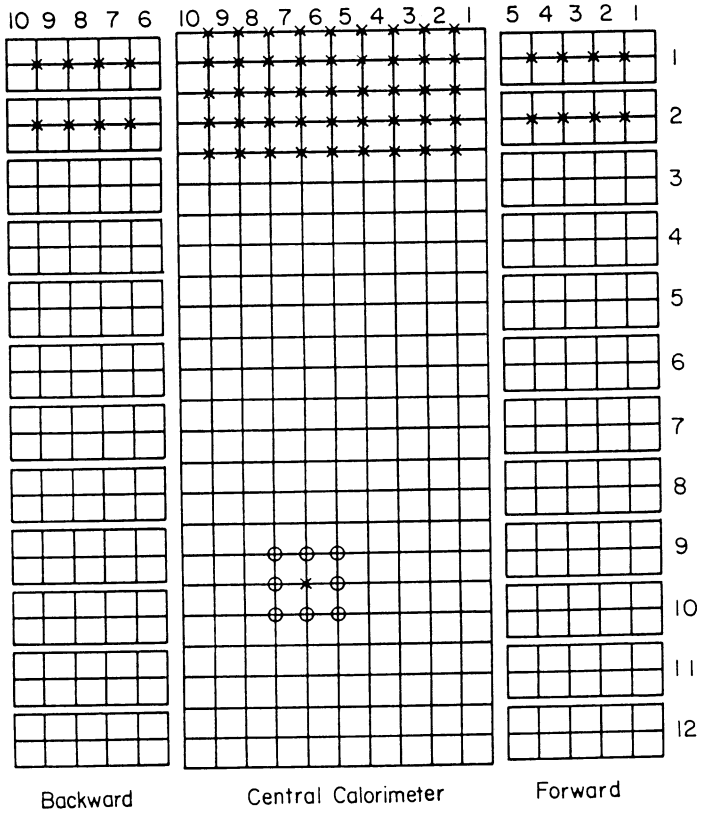

Fig. 4 : Development of the electromagnetic calorimeter cells in the θ-ϕ plane. Crosses in the upper part indicate all clusters of 2 x 2 cells. Circles in the lower part indicate the clusters which are vetoed after a peak (cross) has been detected.

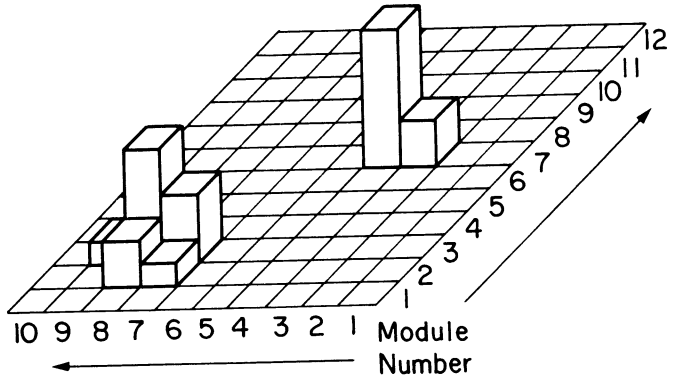

Fig. 5a : Example of energy distribution in the electromagnetic cells with sharing among neighbours.

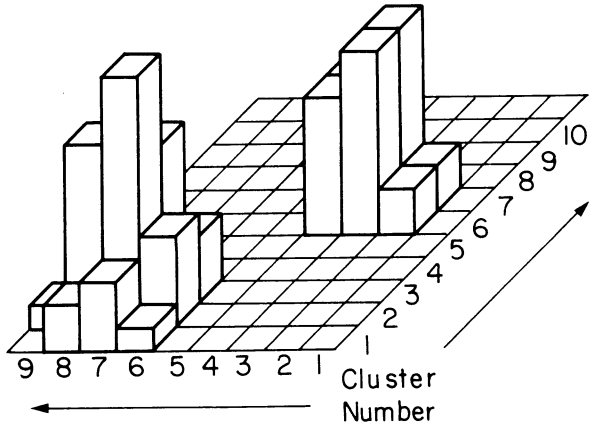

Fig. 5b : Resulting energy distribution among the 2 x 2 clusters.

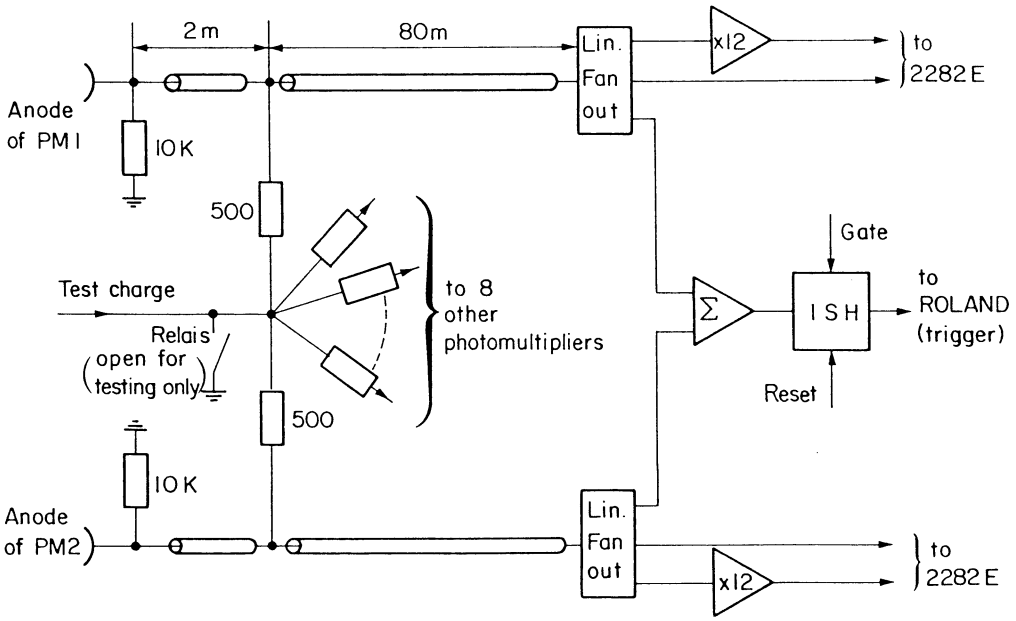

Fig. 6 : The receiver electronics of a single electromagnetic calorimeter cell. The integrating sample-and-hold (ISH) generates a d.c. voltage proportional to the summed charge of the photomultipliers. 20 linear fanouts and 10 ISH form an OLIFAN-module.

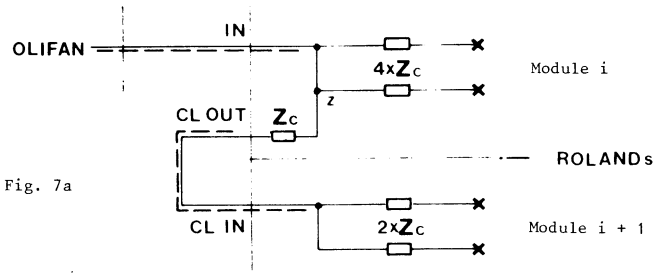

Fig. 7a

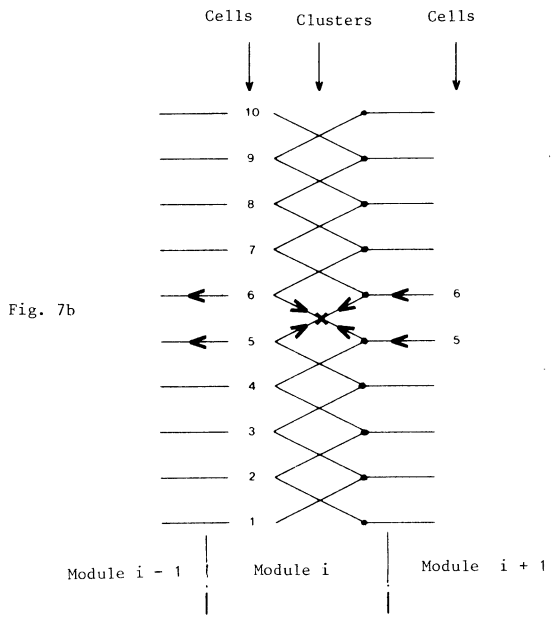

Fig. 7b

Fig. 7 Clustering method at the input of the trigger modules (ROLANDs). $Z_c = 100\Omega$.

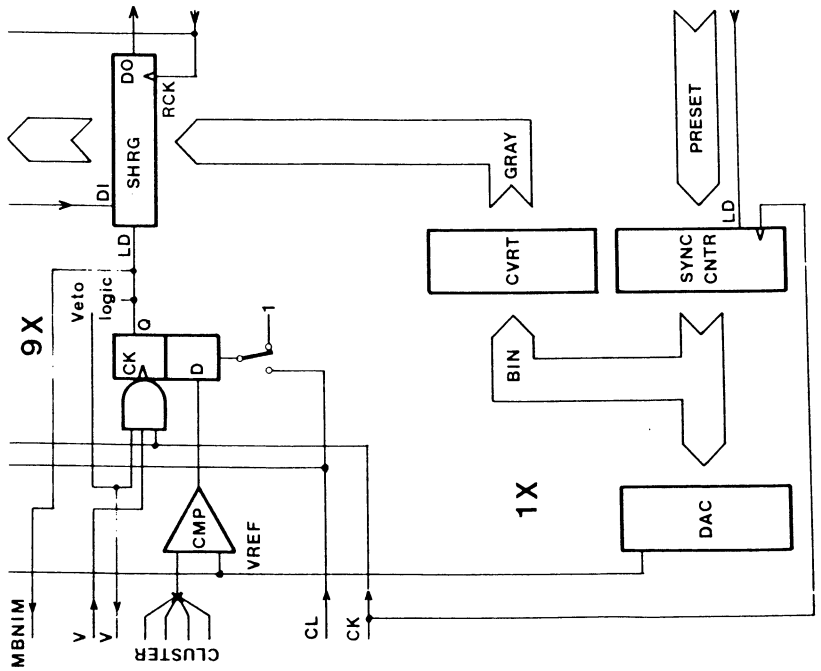

Fig. 9 : Block diagram of ROLAND module. There are 9 comparator-shiftregister circuits and 1 counter-DAC per ROLAND.

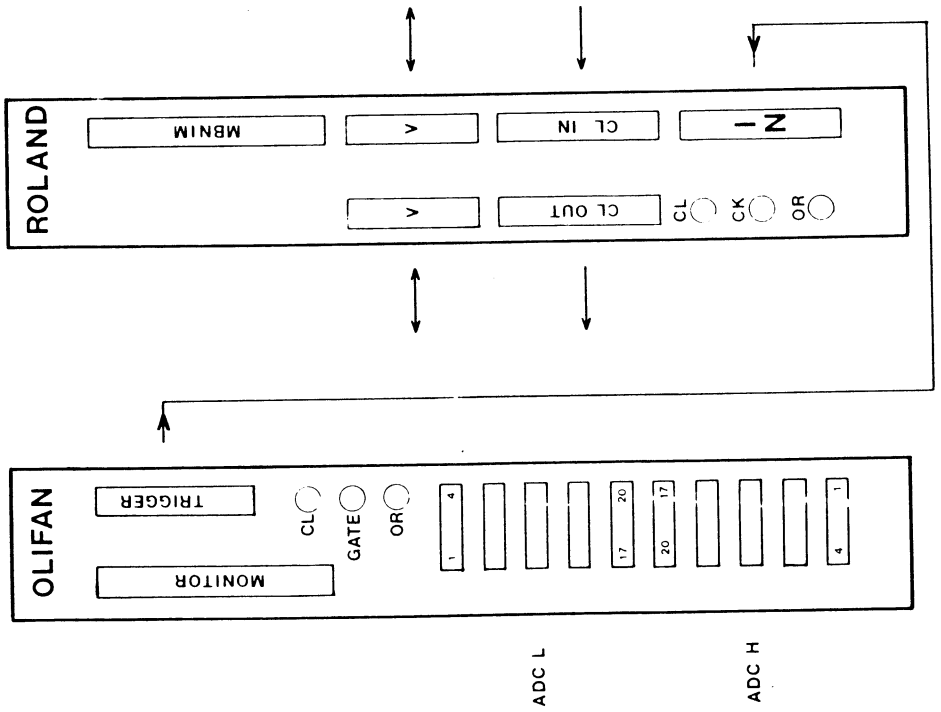

Fig. 8 : Front panels and wiring of the fanout (OLIFAN) and trigger (ROLAND) modules

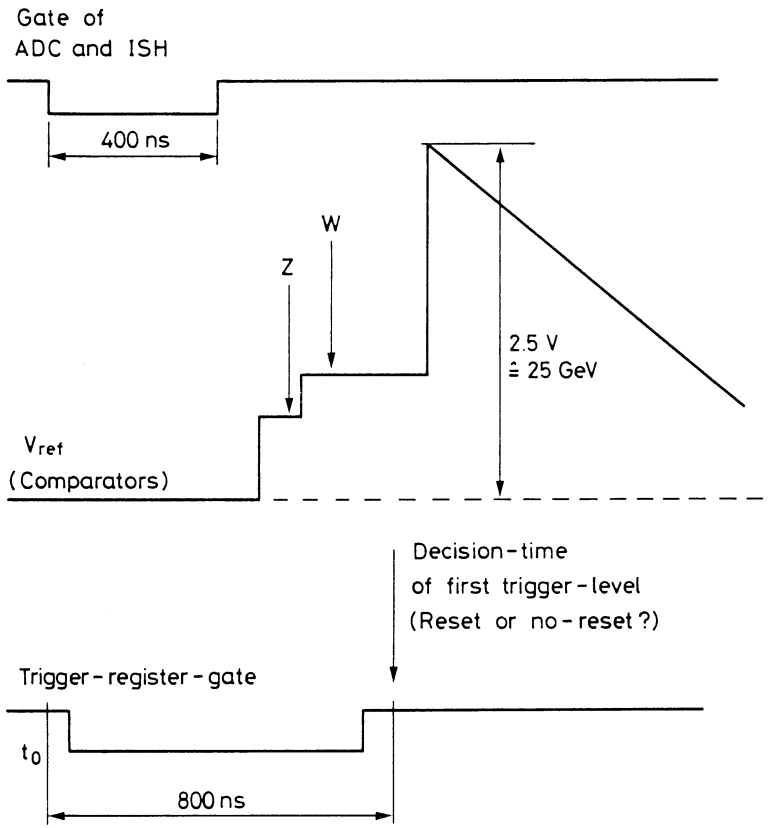

Fig. 10 : Timing of first-level calorimeter trigger.
The V_{ref} conversion slope takes 2.5 µs to return to zero.

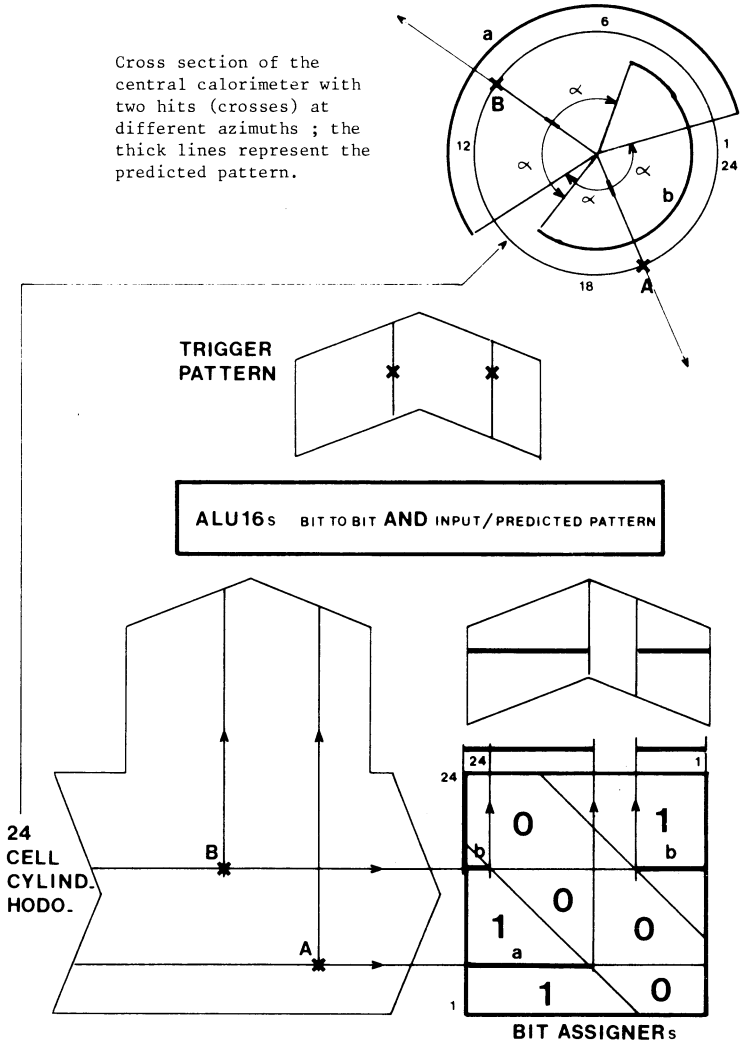

Fig. 11 : Trigger on an electron pair of minimum angular distance using the MBNIM system.

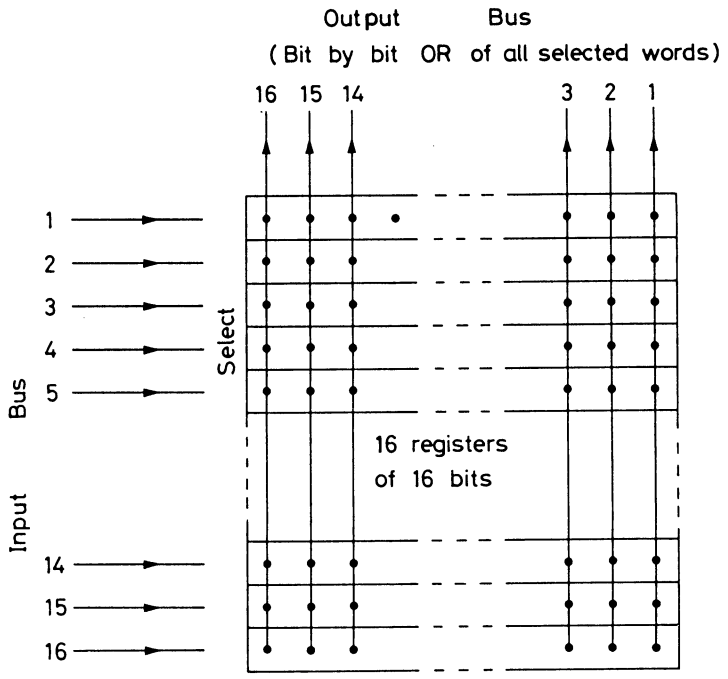

Fig. 12 : Logical diagram of the MBNIM-module BIT-ASSIGNER.

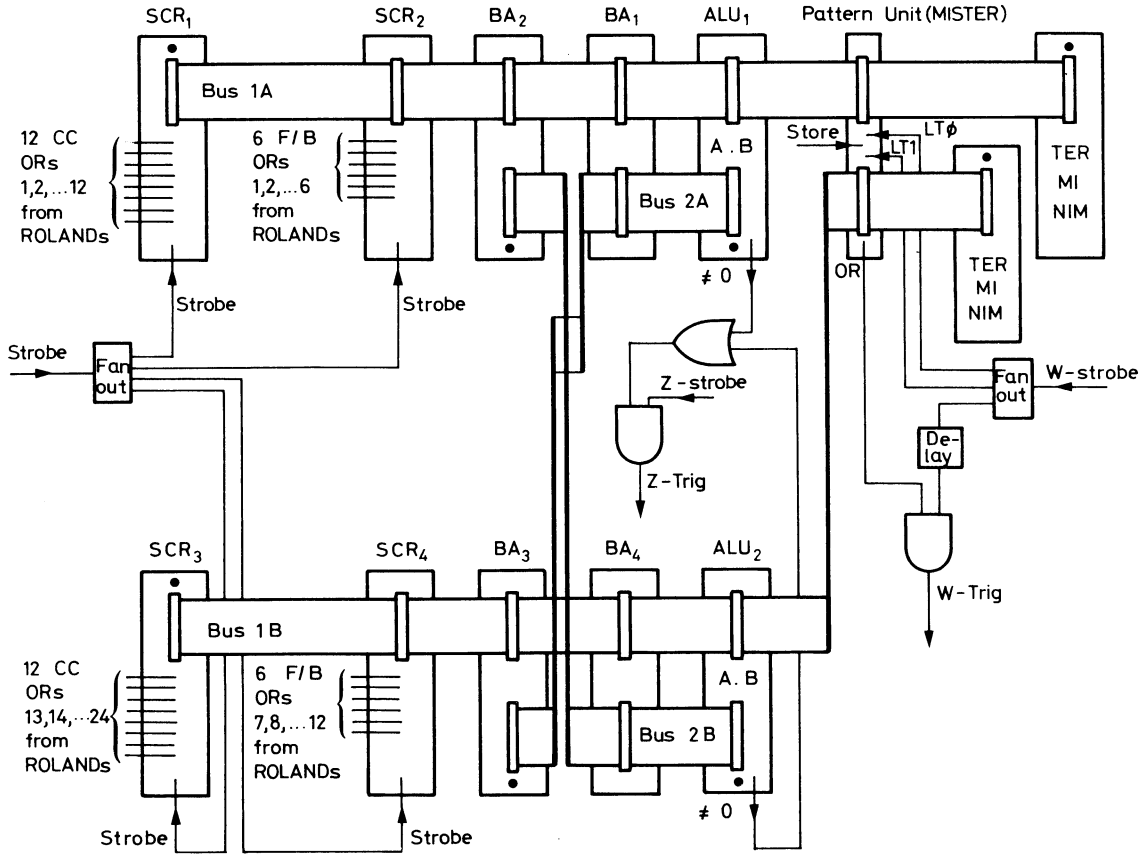

Fig. 13 : The UA2-calorimeter trigger implemented with MBNIM-logic.

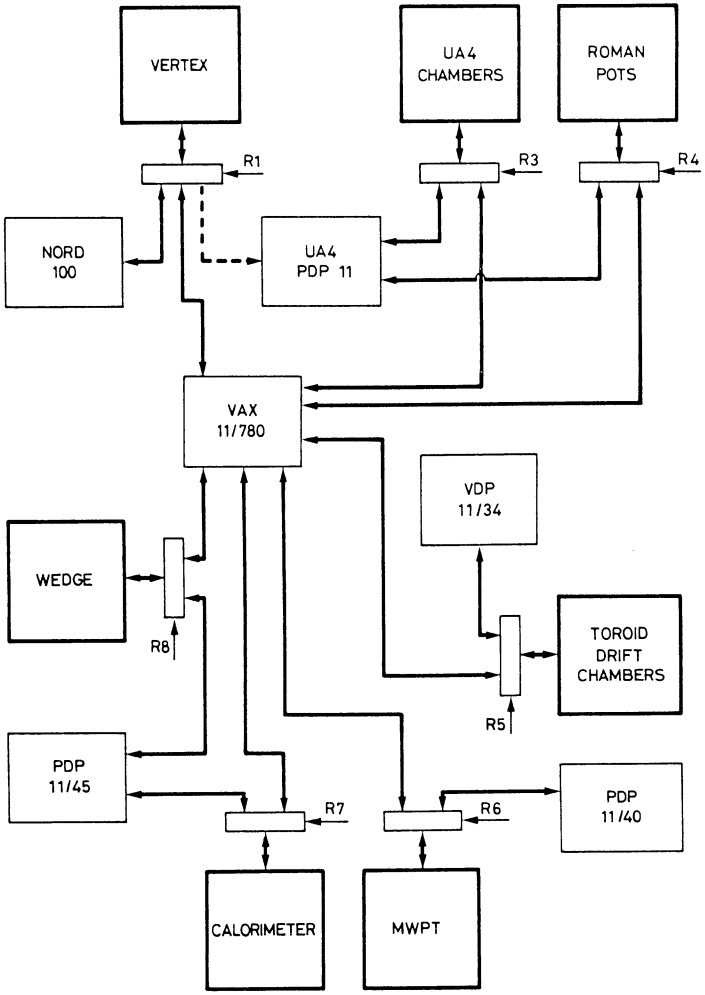

Fig. 14 : Block diagram of UA2/UA4 computers and electronics. The connections are ROMULUS/REMUS cables, the rectangles REMUS-routers.

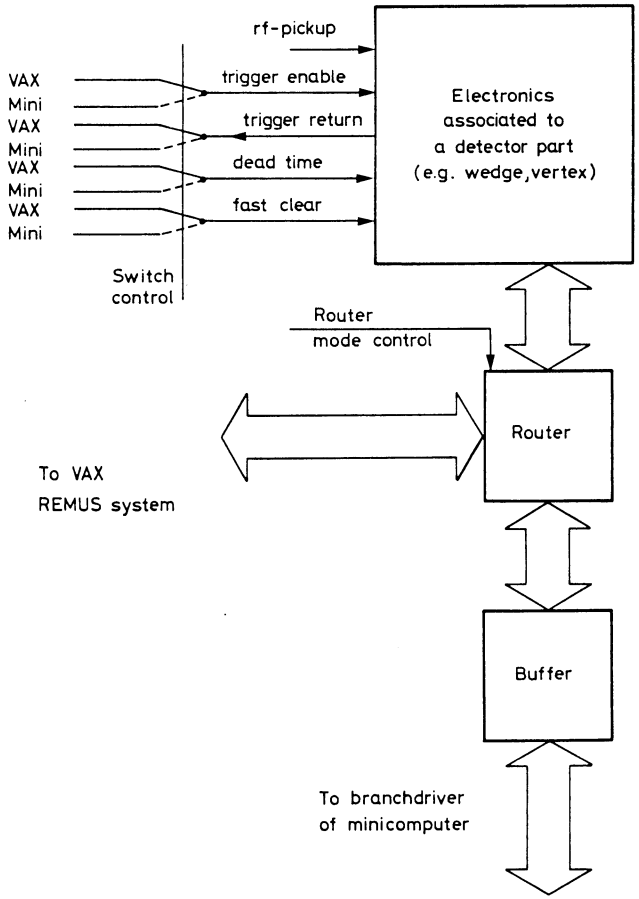

Fig. 15 : Principle of transfer of control between VAX and a minicomputer. "Router mode control" and "switch control" are interlocked.